Low-temperature growth favours hcp structure, flatness and perpendicular magnetic anisotropy of thin (1–5 nm) Co films on Pt(111)

2005 J. Phys.: Condens. Matter 17 5551

(http://iopscience.iop.org/0953-8984/17/36/011)

INSTITUTE OF PHYSICS PUBLISHING JOURNAL OF PHYSICS: CONDENSED MATTER

J. Phys.: Condens. Matter **17** (2005) 5551–5561 doi:10.1088/0953-8984/17/36/011

Low-temperature growth favours hcp structure, flatness and perpendicular magnetic anisotropy of thin (1–5 nm) Co films on Pt(111)

C Quirós[1,2], S M Valvidares[1], O Robach[1,3] and S Ferrer[1,4,5]

[1] European Synchrotron Radiation Facility BP 220, 38043 Grenoble Cedex, France
[2] Departamento de Física, Avenida Calvo Sotelo s/n, Universidad de Oviedo, 33007 Oviedo, Spain
[3] CEA-Grenoble DRFMC/SI3M/PCM, 17 rue des Martyres, 38054 Grenoble Cedex 9, France
[4] ALBA Edifici Ciències, C-3/041 central, UAB, 08193 Bellaterra, Spain

E-mail: ferrer@cells.es

Received 5 May 2005, in final form 28 July 2005
Published 26 August 2005
Online at stacks.iop.org/JPhysCM/17/5551

Abstract

The structural and magnetic properties of thin Co films grown on Pt(111) were investigated *in situ* under UHV using simultaneous surface x-ray diffraction, resonant magnetic surface x-ray diffraction at the Pt L_{III} absorption edge and the surface magneto-optic Kerr effect. We focus on the difference between low-temperature growth and growth at 300 K. Thin (1–5 nm) Co films grown at 120 K (low-T films) have the hcp structure and a small concentration of stacking faults compared to films of the same thickness grown at 300 K (RT films), which contain many stacking faults and have a predominant fcc structure. In addition, the low-T films are flatter. The RT films exhibit a clear reorientation transition of the magnetization, from perpendicular to parallel, at a thickness of 1 nm. In contrast, the low-T films display intense polar Kerr signals up to the largest investigated thickness (5 nm). In these films, the reorientation transition takes place over a large thickness range, through a canted phase. Heating up a low-T film to 300 K induces a rotation of the average easy axis towards the film plane, still with a high polar Kerr signal at 300 K. This behaviour with temperature is mostly reversible. These results are discussed on the basis of the temperature dependence of the anisotropy constants and magnetocrystalline anisotropy differences between the fcc and hcp phases.

1. Introduction

The magnetic anisotropy (MA) of ultra-thin ferromagnetic films is an important physical property for applications in magnetic devices where predetermined easy magnetization axes

[5] Author to whom any correspondence should be addressed.

are required for specific magneto-optical responses. Many combinations of ferromagnetic films and weakly magnetic layers have been investigated in the last decade, searching for most cases perpendicular MA due to its importance in applications. For a review of a large set of experimental results see [1]. In particular, Co/Pt multilayer films show a perpendicular easy magnetization direction and produce relatively large magneto-optical responses. However, in spite of a large amount of research, a detailed understanding of the MA is lacking in many cases, the reason being its enormous sensitivity to structural details. Many transition metal multilayer films prepared with different techniques have (111) surfaces since they are the most stable ones; consequently, the films may exhibit either hcp, fcc or mixed structures depending on the sequence of the stacking. In addition, stacking faults which are inherent to any epitaxial growth process due to kinetic limitations at the usual growth temperatures add structural complexity since they disorder the otherwise regular sequence of planes. Stacking faults may be important in determining the structure of the films since they may act as a sort of nucleation centre for fcc regions in the allotropic transformation of hcp–fcc cobalt [2]. Also, work on CoPtCr thin films for magnetic recording indicates [3, 4] that the stacking faults reduce the magnetic viscosity, which means that moderate magnetic fields may cause substantial demagnetization, which has obviously very important practical consequences.

In this paper we report on the differences between Co films grown at 120 and 300 K on Pt(111). Cobalt deposited at room temperature grows predominantly with the fcc structure and it has many stacking faults. The critical thickness for the change of MA from perpendicular to parallel is in the range 4–6 atomic layers, in agreement with previous findings. However, if grown at ∼120 K, the film adopts the hcp structure and it contains many fewer faults than a film of the same thickness grown at room temperature. The magnetic anisotropy is very different in the two cases: films of 22 atomic layers in thickness still exhibit perpendicular magnetization upon application of moderate perpendicular fields, in strong contrast with films of the same thickness grown at 300 K, which have parallel magnetization under the same applied field. These findings are based on x-ray diffraction, magneto-optical Kerr effect (MOKE) and resonant x-ray scattering measurements.

2. Experimental details

The experiments were done at the surface diffraction beamline ID3 of the ESRF previously described [5]. The Pt crystal was of (111) orientation. We used a hexagonal basis $\mathbf{A}_1$, $\mathbf{A}_2$ and $\mathbf{A}_3$ {A_1 and A_2 equal to the nearest neighbour surface distance $a_0/\sqrt{2}$ and $\mathbf{A}_3$ perpendicular to the surface ($A_3 = \sqrt{3}a_0$, $a_0 = 3.92$ Å)}. Therefore, the reciprocal space axes H and K are in the surface plane and L is perpendicular to the surface plane. The photon energy was set close to the Pt L_{III} atomic absorption edge (11.564 keV). Magnetic measurements were performed by applying a magnetic field created with an electromagnet allowing a maximum intensity of 1400 Oe at the sample position. The sample surface was in a vertical plane and the direction of the applied field made an angle of 10° with the surface of the crystal. In this way the applied field was mostly in the plane of the crystal surface but it also had a small perpendicular component (maximum 200 Oe). A MOKE set-up with horizontal plane of reflection was installed on the vacuum chamber. It consisted of a laser operating at 675 nm, a p-polarizer followed by a photoelastic modulator whose optical axis was at 45° from the p direction, then the sample. The reflected beam went through an analyser at about 45° from the p direction and it was detected with a photodiode. The incident angle was about 55° from the surface of the crystal. The detection was done in a lock-in mode with modulation of the incident polarization. The modulator phase was put at 176° so as to maximize the 2f component. This leads approximately to a modulation between pure p and pure s polarizations in the incident

beam. The resulting 2f signal is a mixture of transverse, polar and longitudinal signals. In practice, the polar signal dominates largely over the in-plane signals [6]; as a consequence, the in-plane signals can therefore be detected only when the perpendicular component of the magnetization stays practically constant during the field cycle.

Resonant magnetic x-ray diffraction measurements could be performed simultaneously with the MOKE measurements in order to investigate the in-plane component of the induced magnetization of the Pt atoms at the interface. The small magnetic diffraction signals were extracted by cycling the magnetic field while measuring the surface diffracted intensity at a well-chosen $(H\,K\,L)$ in which the magnetic intensity is relatively large. Typically 10–15 field cycles were accumulated to obtain correct statistics (total acquisition time around 10–15 min). This collection scheme is an upgrade of that used in our previous works [7, 8]. The magnetic diffraction intensity was quantified with the asymmetry ratio R [7], which is defined as the magnetically sensitive diffracted intensity normalized to the total intensity. Typical measured values of R are within the range 10^{-2}–10^{-3}. Cobalt was deposited with a water-cooled electron bombardment evaporator at a rate of one atomic layer every 46 s. During evaporation the pressure was about 10^{-10} mbar. The sample temperature was measured with a Pt resistor located in the vicinity of the Pt crystal.

Complementary MOKE measurements were performed in a separate UHV system allowing surface preparation and growth. This system offered the advantage of allowing us to apply independently, with two electromagnets, either a pure parallel field (up to 750 Oe) or a pure perpendicular field (up to 1200 Oe) (within a few degrees). Applying a pure perpendicular field was not possible in the main system because of space requirements above the sample for surface x-ray diffraction. The optical set-up of the separate system consisted of a laser, a first polarizer at 45° from the p direction, the modulator with the optical axis along the s direction, the sample, a quarter-wave plate along the s direction, an analyser along the s direction, and the photodiode. The incident angle was 45°. Again the 2f component was measured, and it contained a mixture of polar, longitudinal, and transverse signals.

3. Results

3.1. Structure

As was described in our previous papers [7, 8], Co grows in an imperfect layer-by-layer mode on Pt(111). The in-plane lattice of the Co film has the main crystallographic directions parallel to those of the Pt substrate, and its lattice vector is 0.90 times that of the Pt one, which corresponds to a 9.5% misfit between both lattices. In other words, Co grows relaxed, with its natural interatomic distance. Along the surface normal, the interplanar spacing also corresponds to that of the basal planes of hcp Co or to that of the (111) planes of fcc Co. However, a small residual strain equal to or below the sensitivity of our measurements (approximately 0.3%) cannot be ruled out.

In most cases epitaxial films grown at cryogenic temperatures exhibit larger roughness than films grown at room temperature due to the reduced surface mobility of the deposited atoms. However, several exceptions have been reported such as Pt on Pt(111) [9] and Fe on Ag(100) [10], which grow flatter at low temperatures than at room temperature (RT). Co on Pt(111) is another exception to the rule. Figure 1(a) shows x-ray reflectivity scans for two films deposited under identical conditions except for the temperature of the substrate. The top curve corresponds to a film of ∼22 atomic layers grown and measured at 120 K and the bottom one to a film of similar thickness (within ±5%) at 300 K. The intense peaks at $L = 3$ are bulk Bragg peaks from the Pt substrate. The broader peaks at $L = 3.3$ are Bragg reflections

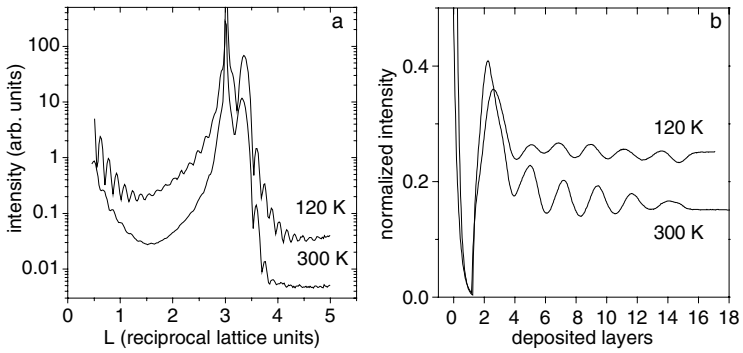

Figure 1. (a) Specular reflectivity of Co films of 22 layers in thickness deposited at room temperature and 120 K. The curves have been vertically shifted for clarity. (b) Temporal evolution of the specular intensity at (0, 0, 1.5) during depositions at two different substrate temperatures.

from the Co planes. As is evident from the figure, the interference fringes arising from the thickness of the film are much more pronounced and abundant in the low-temperature film than in the RT one, indicating higher flatness. A simple evaluation of the rms film roughness gives approximately 1.0 and 1.5 Å for the low-temperature and RT films, respectively.

Additional information on the quality of the films may be derived from figure 1(b), which shows the temporal evolution of the specular intensity at $L = 1.5$. The abscissa axis has been calibrated from measurements of the film thickness as determined from the fringe spacing in the specular scans measured after the growths were completed. In the ordinate axis, the initial intensity before deposition has been normalized to 1.0 in both sets of data. The intensity oscillations are characteristic of a layer-by-layer growth. As is evident from the figure, the specular intensity is higher for the film at 120 K, which confirms its smaller roughness compared to the 300 K film. Numerical simulations (not shown) indicate that the separation of the maxima should correspond to the deposition of two layers for a perfect layer-by-layer growth (the basic reason for the two-layer periodicity arises from the fact that the structure factor of the Co overlayer is about half that of the Pt substrate, which implies that two Co layers are required to obtain the diffracted amplitude of a single Pt layer; see figure 1 in [7] for more details). The positions of the maxima of both curves coincide at the early stages but become separated when the growth proceeds. The data for the low-temperature film show maxima at earlier times than these for the 300 K film. This behaviour is related to the perfection of the film and may be reproduced with numerical simulations. A decrease in mass transport between a layer and the layer underneath shifts the maxima of the oscillations to higher coverage as seen in the 300 K data when compared to the 120 K curve.

A possible explanation for the improved growth at low temperatures follows. Growth at low temperatures tends to produce islands of irregular shapes having large densities of concave corners and kinks compared to room-temperature growth, which usually results in polygonal island shapes [11]. As previously suggested by Lundgren *et al* on low-temperature studies of growth of Co on Pt(111) by STM [12], concave corners and kinks facilitate the descent of atoms from an atomic layer to the layer underneath and therefore enhance the interlayer mass transport and the film flatness compared with the descent from islands with straight steps.

Although this is a good argument that explains our observations, it remains to be understood why the above mechanism is not of general validity since it is well established that in a majority of heteroepitaxial systems the growth quality is worse at low temperatures.

In order to investigate the packing sequence of the Co planes one has to measure L scans with H or K such that $H - K \neq 3n$ (n integer) since the $(00L)$ rod is insensitive. An L

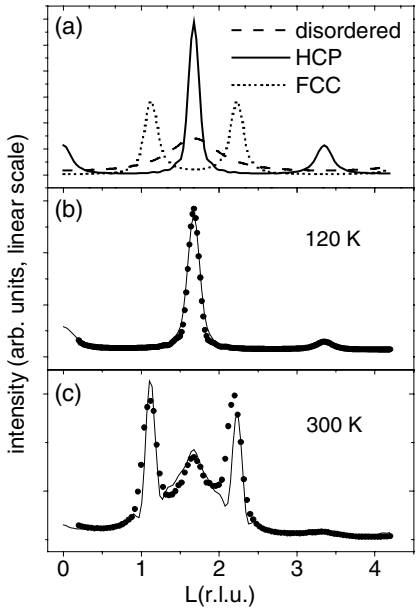

Figure 2. (a) Simulation with the Guinier model of the L scans of the Co film along the (01L) rod for a completely disordered stack and for fcc and hcp stacks with 10% of faults in both cases. (b) The points are the data for a film of 22 atomic layers grown at 120 K and the continuous line is a calculation for hcp packing with 18% of faults. (c) The points are the data for a film of 22 layers grown at room temperature and the continuous line is a fit with 68% of disordered packing, 29% of fcc packing and 3% of hcp packing.

scan at $(H, K) = (0, 1.1)$, which is a position in reciprocal space of a diffraction rod of the Co film, is well suited. That rod is close to the (0, 1) rod of the Pt substrate which exhibits a Bragg peak at $L = 2$. If we call ABCABC the sequence of packing of the (111) planes of the Pt substrate, then a perfect fcc packing of Co planes with the same packing sequence as the substrate would give a peak at $L = 2 \times 1.1 = 2.2$. The twin fcc lattice ACBACB would produce a peak at $L = 1.1$.

If instead of fcc the packing is hcp, then the reflections occur at $L = 1.5 \times 1.1 = 1.65$ and $L = 3.0 \times 1.1$. If the packing is completely disordered and there is only a nearest neighbour interplanar correlation that forces a given plane to be different from the previous and the next ones, then the corresponding diffraction pattern is a single broad peak at $L = 1.5 \times 1.1$.

To estimate the degree of stacking disorder, we analysed the (0, 1.1, L) rods using a model by Guinier [13]. This evaluates the diffracted intensities from an imperfect crystal as a Fourier series with coefficients that depend on the probabilities that two given planes, separated by a certain distance, are identical. These are dependent on the correlations among the crystal planes, which are modelled by introducing disorder parameters on otherwise perfect stacking. These parameters are the probabilities of stacking disorder in hcp or fcc stacking sequences.

As an illustration, figure 2(a) shows the calculated diffracted intensities for complete disordered packing where the only restriction is the dissimilarity of two consecutive planes and for hcp and fcc stacks with 10% stacking disorder each. The effect of an increase on the magnitudes of the disorder parameters is to broaden the peaks and to decrease their maximum intensity. In the fcc stack the two peaks in figure 2(a) correspond to the two possibilities ABCABC and the twin CBACBA, which are equally probable in the model.

Panels (b) and (c) of figure 2 are the experimental data and fits of films of 22 atomic layers grown at 120 and 300 K respectively. The L dependence of the atomic form factor of the Co atoms has been included in the calculation. In (b) the fit corresponds to hcp Co with 18% of faults and in (c) to a film with 68% disordered packing, 29% fcc and 3% hcp.

The advantage of the model is its simplicity and reliability for numerical estimates. As is noticeable in figure 2(c), the fit shows weaker intensity at $L = 2.2$ than at $L = 1.1$ whereas the data show similar intensity. This indicates that from the two fcc packing sequences that of the substrate dominates slightly within the film.

3.2. Magnetism: canted magnetization

The magnetic anisotropy of the Co films was investigated with the MOKE technique by measuring hysteresis cycles. As the applied field made a small angle with the surface, both perpendicular and in-plane magnetization components could be probed. However, as the magneto-optical response for the polar signal is about 30 times larger than that for the transverse one (as determined by us in separate experiments), the latter could only be detected if the polar signal did not change during the field reversal.

Figure 3 shows the MOKE intensities (defined as the magnitudes of the Kerr signal at maximum applied field) versus Co coverage, for films grown at 300 and 120 K. In both cases no magneto-optical signal was detected below 3 atomic layers, probably due to the low Curie temperature for such thin films. The film grown at RT (panel (a)) shows a clear polar Kerr signal at a thickness of 3 layers. It reaches a maximum at 4 layers and then decreases to almost zero at ∼6 atomic layers and above. The transition from 4 to 6 layers corresponds to the change of the easy magnetization axis from perpendicular to parallel. Similar results have been published in the literature in a number of cases, as for example in Co/Au(111) [14], and more recently in Co/Pt(111) [15], which reported widths of the transitions of 2 and 5 layers respectively.

For the RT films, the Kerr signals above 6 layers in figure 3 arise from hysteresis cycles with very small amplitudes corresponding to transverse Kerr effect. Note that between 18 and 22 ML a change in the sign of this transverse Kerr signal occurs. This behaviour follows the typical dependence with thickness of the transverse Kerr signal of Co films on top of nonmagnetic metallic substrates (see figures 4 and 5 in [16]).

Our results for the RT films are in general agreement with the literature [1] and they are well explained with the standard description of the anisotropy of thin films: $E = -K\cos^2\theta$, where E is the anisotropy energy, K the effective anisotropy constant which includes interface and volume terms and the θ angle of the magnetization with the film normal. At the critical film thickness t_c, $K = 0$ since the perpendicular and parallel anisotropies balance. Below t_c the easy direction of magnetization is perpendicular to the film and above it is parallel. From our RT data we obtain $t_c = 5$ atomic layers. Interestingly, the qualitative behaviour shown in figure 3(a) at RT has been repeated in the separate UHV system, as can be seen in figure 3(b). The main difference between both experiments is that at 300 K the signal drops to zero in figure 3(a), while it remains at ∼1/3 of the maximum value in the case of figure 3(b). One possible explanation for this difference is related to the fact that the perpendicular magnetic field is a factor of 6 times weaker in figure 3(a) than in figure 3(b). Anyway, the presence of a critical thickness around 5 atomic layers at 300 K is clear from both set of independent measurements.

The low-temperature data are completely different. At 3 layers there is also a clear Kerr polar signal; it reaches a maximum at about 5 layers and it keeps basically constant for higher thickness up to the maximum measured of 22 atomic layers. If the critical thickness of the film

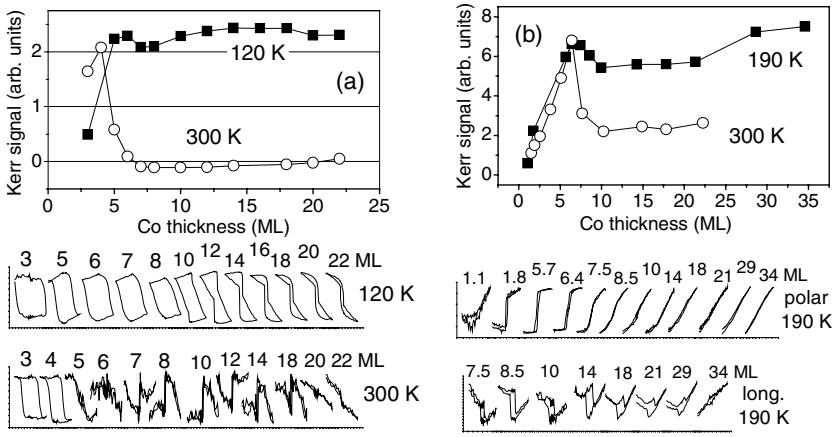

Figure 3. Evolution of the Kerr signal with film thickness for growth temperatures of 120 and 300 K. The measurements were done at the growth temperature. Below are the raw data used to obtain these plots. (a) Data taken with the mixed transverse and polar geometry (in the main system, with a maximum applied field for all the loops around 1300 Oe). The small signals from the 300 K films above 6 atomic layers indicate in-plane magnetization; the scale of the ordinate axis has been increased by a factor of about 20. The larger Kerr signals from the 120 K films arise from perpendicular magnetization. (b) Data taken with the polar geometry (in the separate system). We show the raw data only for the low-T growth (polar, with a maximum applied field for all the loops around 1100 Oe, and longitudinal, with a maximum applied field around 700 Oe).

was above 22 atomic layers, one should expect an approximately linear increase of the Kerr polar signal with coverage since the laser beam probes the whole thickness of the film. The experiment was repeated in the separate system, and basically the same results were obtained; in particular the existence of a maximum at 5 atomic layers was confirmed. The corresponding data for the polar Kerr are shown in figure 3(b).

The behaviour of the low-temperature film can be explained as follows. From 3 to 5 atomic layers the situation is similar to the RT film and the magnetization is perpendicular. Above 5 layers the Kerr intensity almost does not change. Assuming that the polar Kerr signal is proportional to $t2M_{\perp}(H_{\max})$, where t is the film thickness and $M_{\perp}(H_{\max})$ is the perpendicular component of the film magnetization at $H = H_{\max}$, this absence of change of the polar signal on increasing the thickness can be interpreted in two ways:

(i) either the film is saturated along the surface normal at $H = H_{\max}$ and the average saturation magnetization M_s of the film decreases on increasing the film thickness, or
(ii) the average saturation magnetization of the film remains constant and the film is not saturated along the surface normal at $H_{\max}$, i.e. $M_{\perp}(H_{\max}) < M_s$.

Argument (i) is rather unphysical and (ii) is the correct interpretation since polar Kerr measurements performed in the separate system indicated that, above 7.5 ML, the maximum magnitude (1100 Oe) of the pure perpendicular field was effectively too small to saturate the film along the surface normal. However, a closer look to the non-saturated magnetic film reveals a more complex scenario than the one described above.

A precise interpretation of the magnetization of the low-T films is beyond our possibilities since it would require a detailed 3D magnetometry analysis. However, we will describe next some plausible ideas based on our data.

Figure 4 displays a comparison between the Kerr signal and the magnetic diffraction signal, for a Co film of 14 ML thickness grown (and measured) at 120 K. The Kerr cycle (figure 4(a))

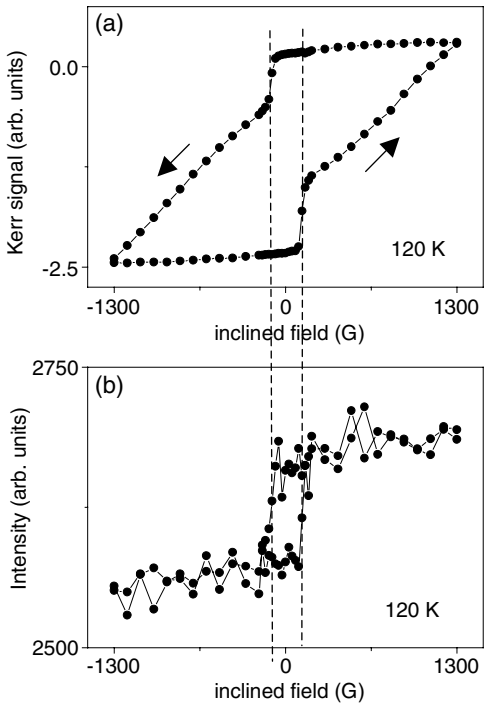

Figure 4. Magnetization loops for a Co film of 14 layers grown at low temperature on Pt(111): measurements with the transverse-polar setup and the inclined magnetic field (10° away from the surface). (a) Kerr signal (polar, $\Delta M_\perp$), (b) resonant diffracted x-ray intensity at (0, 1, 3.6) (sensitive only to the transverse $\Delta M_\parallel$). The dashed lines emphasize that the coercive fields of both square cycles are equal (see text).

has a shape that results from the superposition of two $\Delta M_\perp$ features: a square cycle with a low coercive field of 150 Oe and a non-saturated cycle (slopes of ∼45° in the figure). The magnetic diffraction cycle (figure 4(b)) also shows a superposition of two $\Delta M_\parallel$ features: a square cycle with a low coercive field of 150 Oe and a small additional slope of the plateau. We tentatively interpret these results as a consequence of the existence of a canted magnetization phase. The main argument is the following: the inclined applied field produces a *simultaneous* reversal of both the perpendicular and parallel components of the magnetization of this phase. The reversal of $M_\perp$ creates a square cycle of high amplitude in the Kerr signal. The reversal of the $M_\parallel$ component is not visible on the Kerr signal due to the much lower sensitivity to $\Delta M_\parallel$ compared to $\Delta M_\perp$, but it is clearly visible on the cycles measured by magnetic diffraction, which are sensitive only to the parallel component of the magnetization.

At this point it is worth recalling that the magnetic surface diffraction technique does measure a signal proportional to the parallel magnetization of the Pt atoms at the interface. The element selectivity with respect to the Pt comes from the use of resonant magnetic scattering, i.e. a measurable effect is obtained only when the energy of the incoming x-rays is close to the Pt L_{III} edge. The selectivity of these measurements with respect to the parallel component of the magnetization comes from the polarization of the incident x-ray beam and the scattering geometry, which causes the magnetic part of the diffracted intensity to depend only on $M_\parallel$. In previous studies [7, 8] we found that the Pt magnetization is confined to the interface atoms in contact with Co.

In figure 4(b), the diffracted intensity was measured at $(H, K, L) = (0, 1, 3.6)$ since at this specific place in reciprocal space the magnetic resonant part is intense, about 2% of the total diffracted intensity which is itself relatively small because it is a surface diffraction signal, between two Bragg peaks on a Pt crystal truncation rod.

In our analysis we assumed that the induced magnetization of Pt is parallel to that of Co atoms and that the parallel magnetization of Co is uniform over the film thickness (without necessarily being homogeneous laterally). Within these hypotheses, figure 4(b) can be considered to represent the parallel magnetization cycle of the Co film.

In addition to the canted phase discussed above, another one might exist on the film that would cause the ∼45° slopes in the polar Kerr cycles in figure 4(a) indicated by arrows. It could be a perpendicular easy phase which would be a 'remainder' of the low-thickness perpendicular phase. Its cycles progressively close as thickness increases. Although that phase would be mostly perpendicular, it would also have a small parallel component which is evidenced by the small slopes of $M_{\parallel}$ versus H in figure 4(b) above or below the coercive field. This second phase would grow only at low film thickness and remain basically unchanged in dimensions for coverages above ∼5 ML. Due to this, it would not contribute to the changes of the magnitude of the polar Kerr signal above that coverage (figure 3(a)). In spite of these experimental results, further work is needed to fully evidence and characterize that complex magnetization behaviour.

In conclusion, films grown at low temperature exhibit a behaviour similar to the RT ones below 5 atomic layers; however, above that coverage the magnetization seems to be canted, which indicates that the reorientation transition starts but it has not still been completed at 22 layers.

3.3. Temperature effects

We will now discuss the variations with temperature of the magnetic properties of a thick Co film grown at low temperature (22 ML, 120 K). It is important, in view of applications, to check if the high polar Kerr signal obtained at low temperature is retained when warming the films up to room temperature. When the low-T film was slowly heated to 300 K, the intensity of the polar signal decreased to 40% of its initial value. Subsequent cooling caused a 80% recovery of the initial intensity. Similar but opposite behaviour was observed in the resonant diffracted signal: heating caused an increase of 34% and subsequent cooling caused a decrease to a value 15% higher than the starting one.

The partial irreversibility of the temperature variations could be due to slight irreversible changes of structure on annealing. As described in a previous article [7], heating up a 6 ML low-T film to 300 K produced very little evolution of the film structure, except for a small interdiffusion at the interface. It is worth mentioning here that the inverse experiment of cooling down a 22 ML film grown at RT did not produce measurable polar Kerr signals.

We now discuss the results concerning the (partially) reversible variations of magnetic properties with temperature, in the light of the theoretical approach by Millev *et al* [17]. These authors started from an expression of the free energy of a thin ferromagnetic film:

$$F(\theta) = Kt_1 \sin^2\theta + K_2 \sin^4\theta \tag{1}$$

where θ is the angle between the surface normal $\mathbf{n}$ and the magnetization $\mathbf{M}$,

$$Kt_1 = K_1 - \frac{\mu_0 M^2}{2} \tag{2}$$

and the reference state of zero free energy is the one with $\mathbf{M} \parallel \mathbf{n}$, the film being considered as a structure with uniaxial anisotropy around the surface normal, with first and second order

anisotropy constants K_1 and K_2. They used the standard phenomenological assumption for the dependence of K_1 and K_2 on the thickness and on the bulk (K_{1b}, K_{2b}) and surface/interface (K_{1s}, K_{2s}) anisotropy constants:

$$K_1(d,T) = K_{1b}(T) + 2\frac{K_{1s}(T)}{d}, \tag{3a}$$

$$K_2(d,T) = K_{2b}(T) + 2\frac{K_{2s}(T)}{d}. \tag{3b}$$

From equations (2), (3*a*) and (3*b*), and the boundary condition $K_2(d_2,T) = -Kt_1(d_2)/2$ (see [17] for further details), the following expression for the thickness d_2, at which the thickness-driven reorientation transition finishes, can be written:

$$d_2(T) = \frac{2(2K_{2s} + K_{1s})}{\frac{1}{2}\mu_0 M^2 - (2K_{2b} + K_{1b})}. \tag{4}$$

The denominator in equation (4) can be estimated at various temperatures from the bulk values given in [18] for hcp cobalt: $\frac{1}{2}\mu_0 M^2$, K_{1b} and K_{2b} are approximately 1.31, 0.75 and 0.10 MJ m^{-3} at 120 K and 1.23, 0.5 and 0.12 MJ m^{-3} at 300 K. This leads to 0.36 and 0.49 MJ m^{-3} for the denominator at 120 and 300 K respectively. This simple evaluation is telling us that in hcp Co the denominator decreases when the temperature is lowered. Assuming that K_{1s} and K_{2s} do not vary between 120 and 300 K, this would mean that d_2 is larger at 120 K than at 300 K, i.e. the reorientation transition lasts longer at low temperatures.

This rough estimate of d_2 is consistent with our results on the temperature dependence of the orientation of the 'average' easy axis: for a film with a thickness within the range where the reorientation takes place, changing the value of d_2 to a lower value makes the film progress towards the parallel state, which is what happens to the 22 ML film grown at 120 K when increasing the temperature to 300 K. However, one has to keep in mind that as the film consists most likely of two magnetic phases (as discussed in the previous section), an interpretation based on the analysis of Millev is insufficient since it is based on a homogeneous magnetization.

3.4. Magnetocrystalline anisotropy

We will now discuss the possible structural origins of the differences of magnetic properties induced by differences in the growth temperature (120 or 300 K). The most relevant contributions to the magnetic anisotropy in our films are dipolar E_d, interface and surface K_i and magnetocrystalline K_m. The magneto-elastic contribution may be ignored because the epitaxial films at 300 and 120 K are relaxed and have no strain within our experimental accuracy. The most obvious source of differences is the magnetocrystalline anisotropy. The low-T grown hcp films are uniaxial with a first order anisotropy constant of 0.75 MJ m^{-3} at 120 K favouring perpendicular magnetization. The RT-grown fcc films have a much smaller anisotropy constant: -0.085 MJ m^{-3} [19]; as it is negative, in-plane magnetization is favoured. This large difference allows us to qualitatively understand our findings. The low-T films display a large uniaxial magnetocrystalline anisotropy since they have the hcp structure which causes a non-zero perpendicular magnetization, in spite of the demagnetizing field, even for relatively thick films (22 layers) as discussed above. The RT films are much more isotropic due to both the higher symmetry of the fcc unit cell and the large concentration of stacking faults which increases the symmetry even further. A similar effect of the hcp versus fcc structure on the anisotropy was reported earlier in Co films of $\sim$100 nm in thickness on other substrates [20].

4. Conclusions

In summary, Co films grown at 120 K on Pt(111) are hcp and contain few stacking faults compared to films deposited at room temperature. They produce intense polar signals even for thickness of 4.4 nm, in strong contrast with films grown at room temperature. The most likely explanation is based on the differences of magnetocrystalline anisotropy between the hcp and fcc structures. The reorientation transition in the low-T films is found to occur over a large thickness range, and is not completed at 35 ML. The transition state might consist of a mixture of two phases: a canted phase and an easy-perpendicular phase. The heating of a 22 ML low-T film up to room temperature was also studied. It produces a rotation of the average easy axis of a low-T film towards the parallel direction, which can be explained by a reduction of the thickness of completion of the transition. This interpretation is based on the analysis by Millev *et al* and on the temperature dependence of the bulk magnetic properties of hcp Co. We found that 40% of the polar signal obtained at low T is retained at 300 K.

Acknowledgments

Thanks to E Paiser, L Petit, H Isérn and A Solé for technical assistance. C Quirós acknowledges financial support from the Spanish Government through the 'Ramón y Cajal' program.

References

[1] Johnson M T, Bloemen P J H, den Broeder F J A and de Vries J J 1996 *Rep. Prog. Phys.* **59** 1409
[2] Sort J, Nogues J, Surinach S and Baro M D 2003 *Phil. Mag.* **83** 439
[3] Dova P, Laidler H, O'Grady K, Toney M F and Doerner M F 1999 *J. Appl. Phys.* **85** 2775
[4] Laidler H and Holloway L 2001 *J. Magn. Magn. Mater.* **226** 1633
[5] Ferrer S and Comin F 1995 *Rev. Sci. Instrum.* **66** 1674
[6] Ding H F, Pütter S, Oepen H P and Kirschner J 2001 *Phys. Rev.* B **63** 134425
[7] Robach O, Quirós C, Steadman P, Peters K F, Lundgren E, Alvarez J, Isern H and Ferrer S 2002 *Phys. Rev.* B **65** 054423
Robach O, Quirós C, Steadman P, Peters K F, Lundgren E, Alvarez J, Isern H and Ferrer S 2005 *Phys. Rev.* B **71** 099903 (erratum)
[8] Ferrer S, Alvarez J, Lundgren E, Torrelles X, Fajardo P and Boscherini F 1997 *Phys. Rev.* B **56** 9848
[9] Kunkel R, Poelsema B, Verheij L K and Comsa G 1990 *Phys. Rev. Lett.* **65** 733
[10] Egelhoff W F Jr and Jacob I 1989 *Phys. Rev. Lett.* **62** 921
[11] Zhang Z and Lagally M G (ed) 1998 *Morphological Organization in Eitaxial Growth and Removal* (*Series on Directions in Condensed Matter Physics* vol 14) (Singapore: World Scientific) p 265
[12] Lundgren E, Stanka B, Leonardelli G, Schmid M and Varga P 1999 *Phys. Rev. Lett.* **82** 5068
[13] Guinier A 1994 *X-Ray Diffraction in Crystals, Imperfect Crystals and Amorphous Bodies* (New York: Dover)
[14] Allenspach R, Stampanoni M and Bischof A 1990 *Phys. Rev. Lett.* **65** 3344
[15] Lee J W, Jeong J R, Shin S C, Kim J and Kim S K 2002 *Phys. Rev.* B **66** 172409
[16] Dehesa-Martínez C, Blanco-Gutièrrez L, Vélez M, Díaz J, Alvarez-Prado L M and Alameda J M 2001 *Phys. Rev.* B **64** 024417
[17] Millev Y and Kirschner J 1996 *Phys. Rev.* B **54** 4137
[18] Stearns M B 1986 *Magnetic Properties of 3d, 4d, and 5d Elements, Alloys and Compounds* (*Landolt-Börnstein, New Series*) vol 19a, Group III, ed H P J Wijn (Berlin: Springer)
[19] Hillebrand B, Fassbender J, Jungbut R, Güntherodt G, Roberts D J and Gehring G A 1996 *Phys. Rev.* B **53** R10548
[20] Weller D, Harp G R, Farrow R F C, Cebollada A and Sticht J 1994 *Phys. Rev. Lett.* **72** 2097